

# The epigenetic landscape of transgenerational acclimation to ocean warming

Taewoo Ryu<sup>1,2,5</sup>, Heather D. Veilleux<sup>3,5</sup>, Jennifer M. Donelson<sup>3,4</sup>, Philip L. Munday<sup>1,2,5</sup> <sup>3\*</sup> and Timothy Ravasi<sup>1,2,5</sup> <sup>2\*</sup>

**Epigenetic inheritance is a potential mechanism by which the environment in one generation can influence the performance of future generations<sup>1</sup>. Rapid climate change threatens the survival of many organisms; however, recent studies show that some species can adjust to climate-related stress when both parents and their offspring experience the same environmental change<sup>2,3</sup>. Whether such transgenerational acclimation could have an epigenetic basis is unknown. Here, by sequencing the liver genome, methylomes and transcriptomes of the coral reef fish, *Acanthochromis polyacanthus*, exposed to current day (+0 °C) or future ocean temperatures (+3 °C) for one generation, two generations and incrementally across generations, we identified 2,467 differentially methylated regions (DMRs) and 1,870 associated genes that respond to higher temperatures within and between generations. Of these genes, 193 were significantly correlated to the transgenerationally acclimating phenotypic trait, aerobic scope, with functions in insulin response, energy homeostasis, mitochondrial activity, oxygen consumption and angiogenesis. These genes may therefore play a key role in restoring performance across generations in fish exposed to increased temperatures associated with climate change. Our study is the first to demonstrate a possible association between DNA methylation and transgenerational acclimation to climate change in a vertebrate.**

Acclimation through phenotypic plasticity may buffer populations against the impacts of rapid environmental change and provide time for genetic adaptation to catch up over the longer term<sup>4,5</sup>. Transgenerational acclimation is a form of phenotypic plasticity that occurs when the environment experienced by parents alters the performance of offspring<sup>2–4</sup>. The mechanisms responsible for this type of potentially adaptive phenotypic plasticity are currently unknown, but epigenetic factors are often assumed to be involved<sup>1,6</sup>. Genomic DNA methylation is a mechanism that has been implicated in the transfer of epigenetic information from parents to the next generation in model organisms. For example, DNA methylation could be involved in the case of imprinted genes<sup>7</sup> or the diet-induced paternal effect on the propensity for obesity<sup>8</sup>.

Recently, we have shown that the common reef fish, *Acanthochromis polyacanthus*, can fully acclimate its scope for oxygen consumption (net aerobic scope) when both parents and their offspring experience the same increase in water temperature<sup>2,9</sup>. They do this by changing their transcriptional regulation of metabolism, cytoprotection, immunity, growth and cellular organization.

Furthermore, these fish that are transgenerationally exposed to 3 °C warmer water (transgenerational treatment) differentially express a similar suite of genes compared with fish that are exposed to elevated temperatures from early development for just one generation (developmental treatment), albeit with more genes and higher magnitude changes in expression<sup>9</sup>. Reproductive capacity, however, was impaired in developmental and transgenerational fish, and only improved when temperature was increased incrementally (step-wise treatment) across two generations<sup>10</sup>. Here, we investigate if genomic DNA methylation could be implicated in the observed transgenerational plasticity of *A. polyacanthus* in an ocean warming scenario. We sequenced and systematically analysed the liver genome from an F<sub>1</sub> individual, as well as the methylomes (four individuals per treatment) and transcriptomes (four to five individuals per treatment) of F<sub>2</sub> adult fish exposed throughout life to current day temperatures (+0 °C) or projected future warming (+3 °C) (Fig. 1a, Methods and Supplementary Table 1). Specifically, we assessed four treatment groups: three treatments in which the F<sub>2</sub> fish reared throughout life at +3 °C were from F<sub>1</sub> parents that had experienced either +0 °C, +1.5 °C or +3 °C (developmental, step-wise and transgenerational treatments, respectively), and a control group in which both F<sub>1</sub> and F<sub>2</sub> fish experienced +0 °C (Methods). Previously we analysed the de novo transcriptome for control, developmental and transgenerational treatments<sup>9</sup>; hence, here we focus on the epigenetic regulation of these treatments by assessing the methylomes and how they relate to the acclimating phenotype, net aerobic scope (NAS) and gene expression, with the addition of the step-wise treatment where F<sub>1</sub> fish are reared at +1.5 °C and F<sub>2</sub> fish at +3 °C. We constructed high-quality genome and transcriptome sequences and predicted 25,301 gene models (Methods). Whole-genome bisulfite sequencing data were produced for F<sub>2</sub> adults (two males and two females) from each treatment (control, developmental, step and transgenerational treatments; Fig. 1a), with high coverage depth (34–62×; Supplementary Table 2). By comparing the methylation patterns among these four groups, we identified 2,078, 389 and 5 unique DMRs for CpG, CHH and CHG (H = A, C or T) contexts, respectively (Fig. 1b). The CpG DMRs reside mainly in exons (21.8%), introns (20.9%) and repeats (19.3%) while the CHH DMRs occur mainly in repeats (32.7%), and exons (17.8%) (Fig. 1c, Supplementary Tables 3,4). CHG methylation was not analysed further as there were so few DMRs (Fig. 1b).

CpG DNA methylation patterns were closely associated with the transgenerational temperature exposure experienced by the fish. In particular, the overall pattern of CpG DMRs in transgenerational treatment fish was clearly and significantly distinct from the other

<sup>1</sup>APEC Climate Center, Busan, South Korea. <sup>2</sup>KAUST Environmental Epigenetic Program, Division of Biological and Environmental Sciences & Engineering, King Abdullah University of Science and Technology, Thuwal, Saudi Arabia. <sup>3</sup>ARC Centre of Excellence for Coral Reef Studies, James Cook University, Townsville, Queensland, Australia. <sup>4</sup>School of Life Sciences, University of Technology Sydney, Broadway, New South Wales, Australia. <sup>5</sup>These authors contributed equally: Taewoo Ryu and Heather D. Veilleux. \*e-mail: [philip.munday@jcu.edu.au](mailto:philip.munday@jcu.edu.au); [timothy.ravasi@kaust.edu.sa](mailto:timothy.ravasi@kaust.edu.sa)

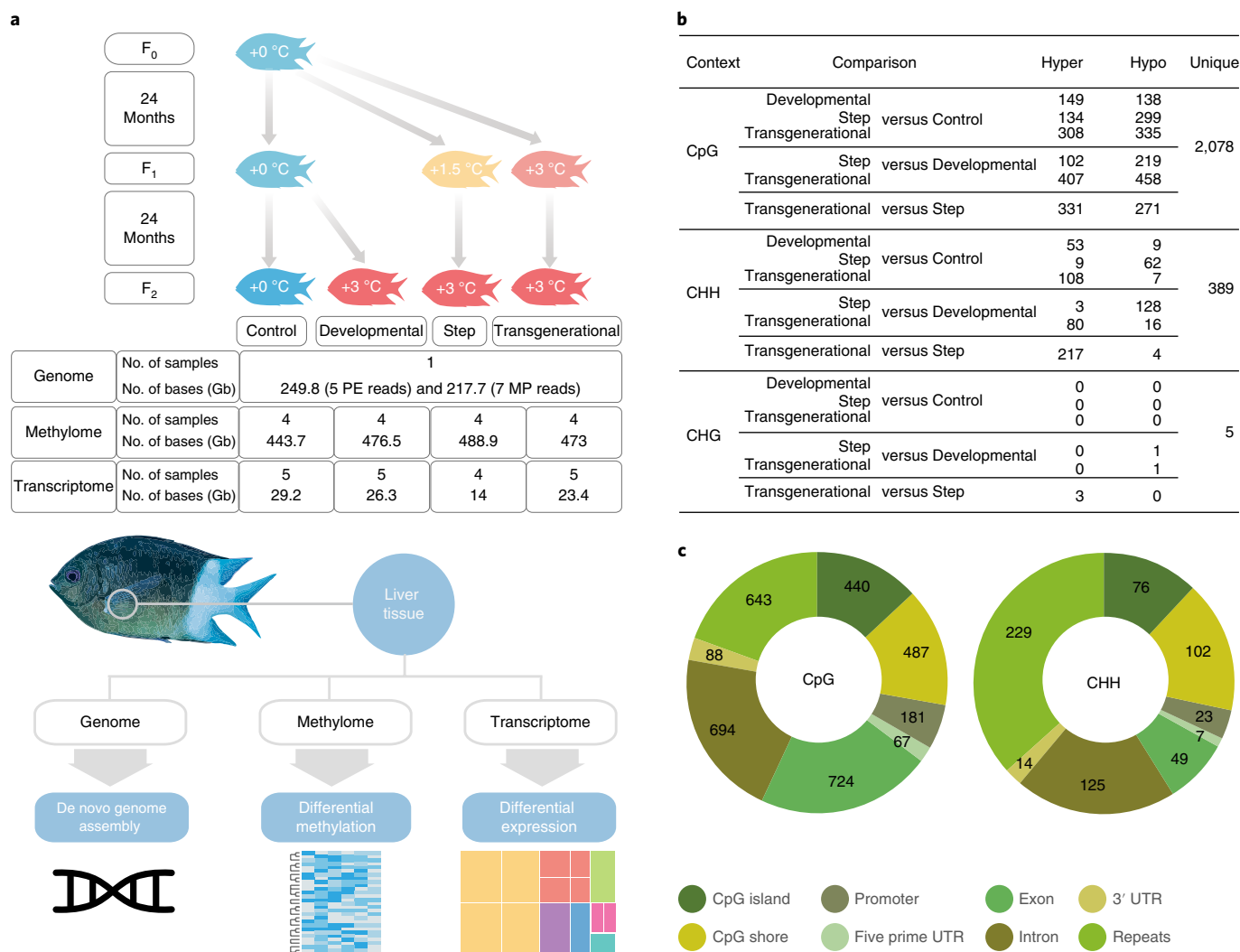


**Fig. 1 | Experimental design and summary of the DMRs. a**, Design of the fish rearing experiment and summary statistics of the genome, methylomes and transcriptomes. **b**, The number of DMRs between treatments for three methylation contexts. Hyper and hypo indicate higher and lower methylation, respectively, in the treatment in the left of the Comparison column compared to the right. The Unique column represents the unique number of DMRs in each methylation context. **c**, DMR distribution across genomic elements for CpG and CHH contexts. The CHG context is not shown due to the low number of DMRs.

treatment groups (Fig. 2a,c) with a more significant change compared to treatments in which the  $F_1$  parents experienced control temperatures (control and development; Supplementary Table 5). Despite all elevated temperature treatments experiencing  $+3^\circ\text{C}$  from hatching, the step treatment had an intermediate level of CpG DMRs compared to developmental and transgenerational treatments relative to control (Fig. 2a,c), consistent with temperatures experienced by their parents (Fig. 1a). Although both transgenerational and step treatments were able to restore aerobic performance at  $+3^\circ\text{C}$  compared to the developmental treatment (Supplementary Table 6), only the step treatment improved reproductive capacity<sup>11</sup>. Thus, step fish did not differentially methylate more CpGs to improve reproductive and aerobic performance, compared to the transgenerational fish that only improved aerobic performance, at least in the liver. This suggests that fish subjected to an incremental exposure of  $+3^\circ\text{C}$  across two generations show a more energy-efficient response to the warmer environment, compared to fish directly exposed to a  $+3^\circ\text{C}$  for two generations. There was some variation among individuals that could not be explained by treatment alone (Fig. 2c). However, it was not due to differences in DMRs between males and females as only the step treatment had a significant

difference between genders (Supplementary Table 5) and this was likely driven by sample S1 being distinct (Fig. 2c). Although there was some evidence of reproductive selection in the  $F_1$  parents of the transgenerational treatment<sup>2</sup> that could contribute to the variation in CpG methylation,  $F_2$  sample selection for the methylome was completed in such a way to maintain similar genetic composition in all treatments. CHH DMRs were less distinct among treatments (Fig. 2b) and had considerable overlap of confidence ellipses in the multidimensional scaling (MDS) plot (Fig. 2d). Therefore, our results suggest that CpG differential methylation serves as a superior indicator of an epigenomic response to elevated temperature in *A. polyacanthus* compared with CHH differential methylation. As such, we focused further analysis on the genes that were closest to each CpG DMR, hereafter referred to as differentially methylated genes (DMGs).

Our previous study shows that NAS, a measure of the total capacity for oxygen consumption above resting metabolic rate, is diminished when fish develop at projected future ocean temperatures, but is fully restored in fish that are reared transgenerationally at a higher temperature<sup>2</sup>. Therefore, we sought to identify epigenetically regulated genes involved in this restoration by correlating NAS to the

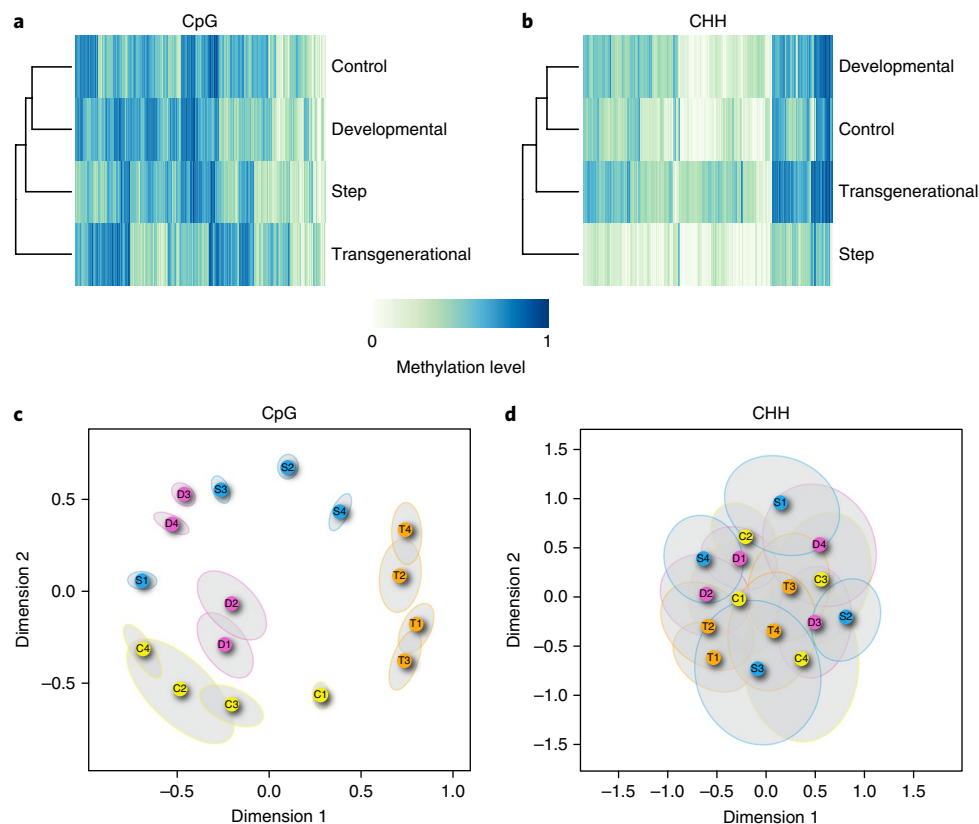


**Fig. 2 | Differential methylation patterns.** **a,b**, Heatmap of DMRs for CpG (**a**) and CHH (**b**) contexts. **c,d**, MDS plot of DMRs for CpG (**c**) and CHH (**d**) contexts. Each coloured circle represents one fish sample and treatment groups are denoted by different colours. C, D, S and T represent control, developmental, step and transgenerational treatments, respectively. Each ellipse represents a 95% confidence region from 1,000 bootstrapping of DMRs from each sample. Non-overlapping ellipses implies statistically significant differences among samples.

methylation levels of the DMRs. Of the 2,078 CpG DMRs associated with 1,563 genes (Supplementary Fig. 1), the methylation levels of 251 DMRs (193 genes) were significantly correlated with standardized NAS from the same fish (Methods and Supplementary Table 7). 64% of the DMGs were negatively correlated to NAS (Fig. 3a) and 36% were positively correlated (Fig. 3b). The majority of negatively NAS-correlated genes were involved in cell organization (20%), metabolism (14%) and transport (10%) (Supplementary Table 7). Similarly, the main functions associated with the positively NAS-correlated genes were cell organization (16%) and metabolism (13%), and also transcription/translation (13%) and stress-related (12%) functions. We found that many of these NAS-correlated and DMGs may play key roles in the epigenetic control of transgenerational thermal acclimation, with functions related to insulin response, energy homeostasis, thermogenesis, mitochondrial activities, hypoxia and vascular functions.

Functions related to energy homeostasis, such as insulin response, nutrient metabolism, mitochondrial activities and oxygen consumption, were highly prominent among differentially methylated and NAS-correlated genes (48 of 193 genes, Supplementary Table 7). At least 22 of these genes mediate insulin secretion, sensitivity, action and signalling, and five are regulated by insulin (Supplementary Table 7). Insulin is the principal regulator of nutrient metabolism and energy control by stimulating glucose uptake into liver, adipose and muscle cells to store into glycogen or fats<sup>11</sup>. Thus, epigenetically regulating insulin may be critical for improved aerobic performance across generations when exposed to increased temperatures. Another means of achieving energy homeostasis is by regulating mitochondria, which are the primary generators of the cellular energy currency, ATP, through aerobic respiration<sup>12</sup>. Twenty-five

differentially methylated and NAS-correlated genes have roles in mitochondrial regulation, respiration, apoptosis, homeostasis and protection (Supplementary Table 7). One gene with a key role in regulating energy balance that was differentially methylated and positively correlated to NAS was *trpm2* (Fig. 4a). Its encoded protein, TRPM2, regulates insulin secretion, energy expenditure and glucose metabolism; can lead to mitochondrial fission and dysfunction when exposed to reactive oxygen species or high glucose; and functions as a molecular thermosensor<sup>13</sup> (Supplementary Table 7). Another gene with a role in energy homeostasis that was differentially methylated and NAS-correlated was *pctp* (Fig. 4b). Its encoded protein, PCTP, is a putative modulator of hepatic metabolism and energy utilization for nutrient homeostasis and, based on transgenic mice models, may be related to broad functions such as insulin sensitivity, thermogenesis, oxygen consumption and mitochondrial activities (reviewed in ref.<sup>14</sup>). Additionally, *CIDEA*, which is involved in lipid storage and insulin sensitivity<sup>15</sup>, was negatively correlated to NAS and had less methylation in control and step fish compared to developmental fish (Fig. 4c and Supplementary Table 7). Furthermore, mice lacking the *cidea* gene showed higher oxygen consumption, metabolic rates and body temperature<sup>16</sup>, indicating that upregulation of this gene could help fish acclimate metabolism and oxygen demand at higher temperatures. Our results indicate that metabolic reprogramming through intensive epigenetic control of insulin and mitochondrial function may be an essential process to maintain metabolic function and energy balance in a warmer environment.

Failure of the cardiovascular system to deliver sufficient oxygen to meet the increased demand of tissues at higher temperatures is hypothesized to set the limits of thermal tolerance in fish and other

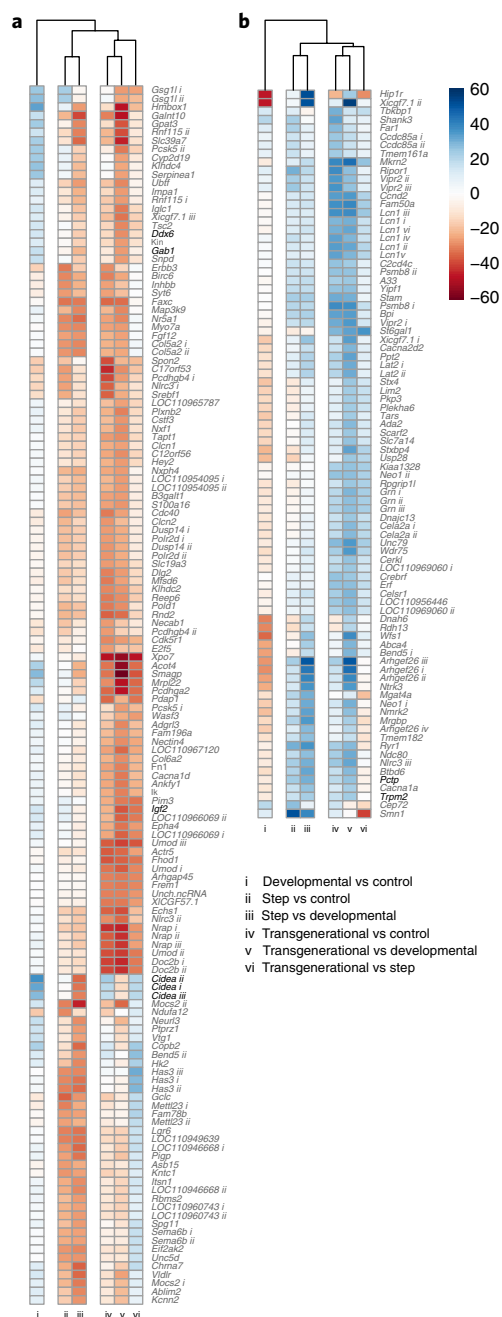


**Fig. 3 | Heatmaps of differentially methylated and net aerobic scope-correlated genes. a, b.** Negatively (a) and positively (b) correlated differentially methylated genes (adjusted  $p < 0.05$ ;  $>25\%$  difference in methylation between treatments) from *A. polyacanthus*, comparing control, developmental, transgenerational and step treatments. Genes described in the text are marked in bold. The colour scale indicates the per cent difference in methylation between two treatments.

ectotherms<sup>17</sup>. Organisms can potentially improve oxygen delivery through angiogenesis, the formation of new blood vessels by sprouting or splitting from existing vasculature<sup>18</sup>. Previously studies have shown that there is epigenetic regulation of angiogenic gene expression due to metabolic flux (reviewed in ref.<sup>18</sup>). In our study, eight genes involved in many processes of angiogenesis were NAS-correlated and differentially methylated (Supplementary Table 7). For example, *gab1*, which encodes a regulatory component of endothelial cell motility that is essential for angiogenesis<sup>19</sup>, was hypomethylated in transgenerational fish relative to developmental fish

(Fig. 4d). In addition, two genes, *igf2* and *ddx6*, contribute to angiogenesis by up- or downregulating vascular endothelial growth factor, a major contributor to angiogenesis<sup>20,21</sup> (Fig. 4e,f). Furthermore, GAB1 functions to balance hepatic insulin sensitivity as a negative modulator<sup>22</sup> and DNA methylation of IGF2 affects transgenerational glucose intolerance<sup>23</sup>, suggesting their multifunctional roles in transgenerational acclimation. Therefore, our data suggests that epigenetic regulation of genes related to adjusting the circulatory system through angiogenesis and counteracting against oxygen fluctuation may lead to improved transgenerational aerobic function.

Unlike most genes where alleles from both parents are expressed, genomic imprinting maintains parental-specific methylation causing only one allele from one parent to be expressed<sup>7</sup>. In humans, prenatal maternal condition, such as stress and famine, can lead to altered *igf2* methylation<sup>24</sup>, a well-studied imprinting gene that encodes the insulin-like growth factor 2 hormone. In fishes, *igf2* plays an important role in promoting growth during development<sup>25</sup> and a genomic imprinting mechanism at the *igf2* locus was reported in goldfish<sup>26</sup>, supporting a regulatory role of DNA methylation across generations in fish. Here we found that *igf2* had significantly lower methylation in the transgenerational treatment compared with control ( $-22\%$ ), developmental ( $-37\%$ ) and step ( $-32\%$ ) treatments (Supplementary Table 7). Thus, experiencing  $+3.0^{\circ}\text{C}$  for two generations significantly altered the methylation of *igf2*. By contrast, the step treatment did not have reduced *igf2* methylation, which may be because the gradual increase in temperature was not as stressful and/or alternative pathways were used to improve condition. This finding warrants further investigation as the reduced *igf2* methylation in transgenerational fish could be a putative parental imprinting mechanism in *A. polyacanthus* to improve performance where both parent and offspring experience the same elevated temperatures.

Of the 1,563 DMGs identified in this study, only 34 were also differentially expressed (Supplementary Fig. 1; Supplementary Table 8). This is consistent with other recent studies reporting a weak correlation between whole-genome differential methylation and gene expression<sup>27</sup>. In our study, the differentially methylated and expressed genes encompassed a wide range of functions mainly involved in cell integrity and organization, regulation of gene and protein expression, growth and development, and transport, and were primarily differentially regulated between the transgenerational and control treatments (Supplementary Table 8; Supplementary Fig. 2). Of particular interest are two mitochondrial genes, *gls2* and *higd1a*, that were hypomethylated and downregulated in the step treatment compared with control fish. These genes are involved in oxygen consumption and control of ATP levels<sup>28</sup>, and the mitochondrial respirasome (supercomplexes of multiple respiratory chain complexes) formation<sup>29</sup>, respectively. Suppression of mitochondrial respiration and hypometabolism was previously implicated in warm acclimation<sup>30</sup> and our results provide molecular evidence for this phenomenon. Additionally, *esrrg*, a master regulator of oxidative capacity and mitochondrial function<sup>31</sup>, was hypermethylated and upregulated in transgenerational compared with developmental fish, suggesting it is likely associated with improved aerobic capacity in transgenerational fish<sup>9</sup>. However, with so few DMGs also differentially expressed, there is likely an additional layer of epigenetic control affecting the expression of these genes, such as histone modification or non-coding RNAs. Furthermore, we postulate that the limited number of differentially expressed DMR genes may be due to alternative pre-mRNA splicing<sup>32</sup> or the developmental stage at which sampling occurred; DMGs may affect expression early in life to establish baseline levels of proteins for continued persistence in that condition and then transcripts return to control levels. In this instance, the few genes that remain differentially expressed when the fish reaches maturity are likely to be necessary for sustaining the animal at the new temperature throughout life.



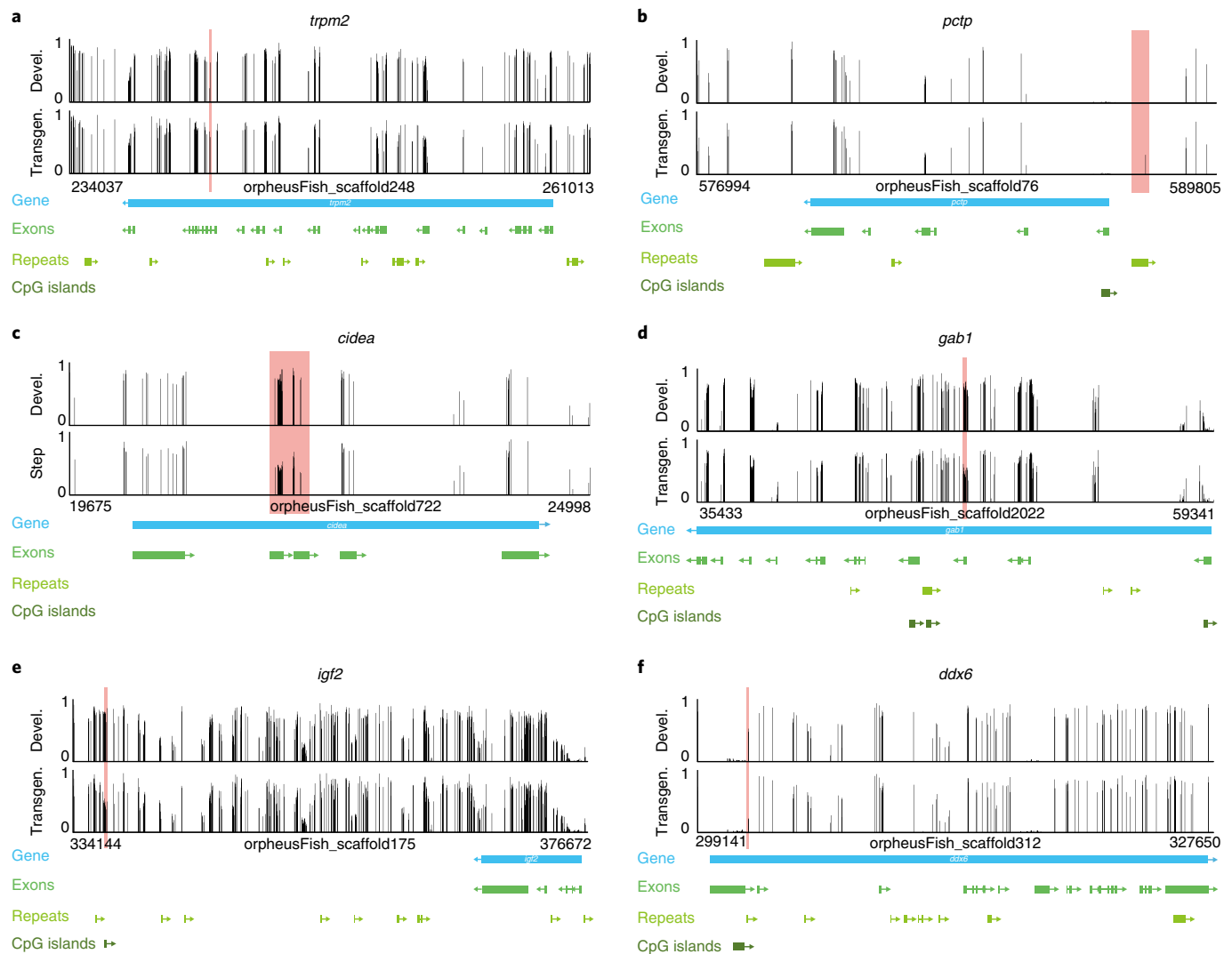


**Fig. 4 | DNA methylation patterns for thermal acclimation.** **a–f**, Density of methylcytosines from the CpG context are shown for selected genes: *trpm2* (**a**), *pctp* (**b**), *cidea* (**c**), *gab1* (**d**), *igf2* (**e**) and *ddx6* (**f**). Red rectangles represent differentially methylated regions. Genomic locations are indicated below the density plot. Gene models are shown for the corresponding coordinates.

In conclusion, our study indicates that the epigenome is altered following exposure to increased temperatures via DNA methylation of specific loci. Although our results are consistent with transgenerational epigenetic effects, we cannot exclude a role for developmental epigenetic effects during the gamete and embryonic stage because eggs experienced the parental conditions until hatching. To conclusively demonstrate transgenerational epigenetic inheritance, future experiments should test if differential methylation and gene expression is retained when fish exposed transgenerationally to high temperature are returned to ambient control conditions in both parental and offspring generations. Nevertheless, we identified 193 DMGs that correlate to aerobic performance, of which many play key roles in metabolic homeostasis, insulin sensitivity and improved oxygen delivery, thus suggesting that these are the core genes associated with physical acclimation to heat stress across generations. Our study shows that exposure to higher temperatures associated with climate change causes genome-wide changes in DNA methylation, demonstrating that epigenetic regulation is possible in a coral reef fish facing a warming ocean, and that DNA methylation could play a role in transgenerational acclimation.

## Methods

Methods, including statements of data availability and any associated accession codes and references, are available at <https://doi.org/10.1038/s41558-018-0159-0>.

Received: 2 March 2017; Accepted: 10 April 2018;

Published online: 30 April 2018

## References

- Jablonka, E. & Raz, G. Transgenerational epigenetic inheritance: prevalence, mechanisms, and implications for the study of heredity and evolution. *Q. Rev. Biol.* **84**, 131–176 (2009).
- Donelson, J., Munday, P., McCormick, M. & Pitcher, C. Rapid transgenerational acclimation of a tropical reef fish to climate change. *Nat. Clim. Change* **2**, 30–32 (2012).
- Salinas, S. & Munch, S. B. Thermal legacies: transgenerational effects of temperature on growth in a vertebrate. *Ecol. Lett.* **15**, 159–163 (2012).
- Munday, P. L., Warner, R. R., Monro, K., Pandolfi, J. M. & Marshall, D. J. Predicting evolutionary responses to climate change in the sea. *Ecol. Lett.* **16**, 1488–1500 (2013).
- Chevin, L. M., Lande, R. & Mace, G. M. Adaptation, plasticity, and extinction in a changing environment: towards a predictive theory. *PLoS Biol.* **8**, e1000357 (2010).

6. Bonduriansky, R., Crean, A. J. & Day, T. The implications of nongenetic inheritance for evolution in changing environments. *Evol. Appl.* **5**, 192–201 (2012).
7. Daxinger, L. & Whitelaw, E. Understanding transgenerational epigenetic inheritance via the gametes in mammals. *Nat. Rev. Genet.* **13**, 153–162 (2012).
8. Ng, S. F. et al. Chronic high-fat diet in fathers programs beta-cell dysfunction in female rat offspring. *Nature* **467**, 963–966 (2010).
9. Veilleux, H. D. et al. Molecular processes of transgenerational acclimation to a warming ocean. *Nat. Clim. Change* **5**, 1074–1078 (2015).
10. Donelson, J. M., Wong, M., Booth, D. J. & Munday, P. L. Transgenerational plasticity of reproduction depends on rate of warming across generations. *Evol. Appl.* **9**, 1072–1081 (2016).
11. Rui, L. Energy metabolism in the liver. *Compr. Physiol.* **4**, 177–197 (2014).
12. Das, J. The role of mitochondrial respiration in physiological and evolutionary adaptation. *Bioessays* **28**, 890–901 (2006).
13. Kashio, M. & Tominaga, M. The TRPM2 channel: A thermo-sensitive metabolic sensor. *Channels* **11**, 426–433 (2017).
14. Kang, H. W., Wei, J. & Cohen, D. E. PC-TP/StARD2: of membranes and metabolism. *Trends Endocrinol. Metab.* **21**, 449–456 (2010).
15. Puri, V. et al. Cidea is associated with lipid droplets and insulin sensitivity in humans. *Proc. Natl Acad. Sci. USA* **105**, 7833–7838 (2008).
16. Zhou, Z. et al. Cidea-deficient mice have lean phenotype and are resistant to obesity. *Nat. Genet.* **35**, 49–56 (2003).
17. Portner, H. O. & Farrell, A. P. Physiology and climate change. *Science* **322**, 690–692 (2008).
18. Fraisl, P., Mazzone, M., Schmidt, T. & Carmeliet, P. Regulation of angiogenesis by oxygen and metabolism. *Dev. Cell* **16**, 167–179 (2009).
19. Laramee, M. et al. The scaffolding adapter Gab1 mediates vascular endothelial growth factor signaling and is required for endothelial cell migration and capillary formation. *J. Biol. Chem.* **282**, 7758–7769 (2007).
20. Chao, W. & D'Amore, P. A. IGF2: epigenetic regulation and role in development and disease. *Cytokine Growth F. Rev.* **19**, 111–120 (2008).
21. de Vries, S. et al. Identification of DEAD-box RNA helicase 6 (DDX6) as a cellular modulator of vascular endothelial growth factor expression under hypoxia. *J. Biol. Chem.* **288**, 5815–5827 (2013).
22. Bard-Chapeau, E. A. et al. Deletion of Gab1 in the liver leads to enhanced glucose tolerance and improved hepatic insulin action. *Nat. Med.* **11**, 567–571 (2005).
23. Ding, G. L. et al. Transgenerational glucose intolerance with Igf2/H19 epigenetic alterations in mouse islet induced by intrauterine hyperglycemia. *Diabetes* **61**, 1133–1142 (2012).
24. Vangeel, E. B. et al. DNA methylation in imprinted genes IGF2 and GNASXL is associated with prenatal maternal stress. *Genes Brain Behav.* **14**, 573–582 (2015).
25. Gabillard, J. C., Rescan, P. Y., Fauconneau, B., Weil, C. & Le Bail, P. Y. Effect of temperature on gene expression of the Gh/Igf system during embryonic development in rainbow trout (*Oncorhynchus mykiss*). *J. Exp. Zool. A* **298**, 134–142 (2003).
26. Xie, B., Zhang, L., Zheng, K. & Luo, C. The evolutionary foundation of genomic imprinting in lower vertebrates. *Chin. Sci. Bull.* **54**, 1354 (2009).
27. Lou, S. et al. Whole-genome bisulfite sequencing of multiple individuals reveals complementary roles of promoter and gene body methylation in transcriptional regulation. *Genome Biol.* **15**, 408 (2014).
28. Hu, W. et al. Glutaminase 2, a novel p53 target gene regulating energy metabolism and antioxidant function. *Proc. Natl Acad. Sci. USA* **107**, 7455–7460 (2010).
29. Vukotic, M. et al. Rcf1 mediates cytochrome oxidase assembly and respirasome formation, revealing heterogeneity of the enzyme complex. *Cell Metab.* **15**, 336–347 (2012).
30. Chung, D. J. & Schulte, P. M. Mechanisms and costs of mitochondrial thermal acclimation in a eurythermal killifish (*Fundulus heteroclitus*). *J. Exp. Biol.* **218**, 1621–1631 (2015).
31. Rangwala, S. M. et al. Estrogen-related receptor gamma is a key regulator of muscle mitochondrial activity and oxidative capacity. *J. Biol. Chem.* **285**, 22619–22629 (2010).
32. van den Hoogenhof, M. M., Pinto, Y. M. & Creemers, E. E. RNA splicing: regulation and dysregulation in the heart. *Circ. Res* **118**, 454–468 (2016).

## Acknowledgements

This study was supported by the Competitive Research Funds OCRF-2014-CRG3-62140408 from the King Abdullah University of Science and Technology. This project was completed under JCU Ethics A1233 and A1415. T.Ryu acknowledges the support from the APEC Climate Center. P.L.M. was supported by the Australian Research Council (ARC) and P.L.M., H.D.V. and J.M.D. were supported by the ARC Centre of Excellence for Coral Reef Studies. We thank C. Ortiz Alvarez and E. J. Steinig (James Cook University) for assisting genomic DNA extraction for methylome sequencing. Figures were enhanced by I. Gromicho, scientific illustrator at King Abdullah University of Science and Technology (KAUST).

## Author contributions

J.M.D. managed the fish rearing experiments and performed metabolism experiments. H.D.V. prepared samples for sequencing. H.D.V. extracted nucleic acids for genome and transcriptome. T.Ryu extracted nucleic acids for methylome sequencing. T.Ryu, H.D.V. and J.M.D. selected samples for sequencing. T.Ryu designed and performed the computational analysis. T.Ryu and H.D.V. interpreted the results. T.Ryu, T.Ravasi, P.L.M., H.D.V. and J.M.D. wrote the manuscript. T.Ravasi and P.L.M. supervised the overall project.

## Competing interests

The authors declare no competing interests.

## Additional information

**Supplementary information** is available for this paper at <https://doi.org/10.1038/s41558-018-0159-0>.

**Reprints and permissions information** is available at [www.nature.com/reprints](http://www.nature.com/reprints).

**Correspondence and requests for materials** should be addressed to P.L.M. or T.R.

**Publisher's note:** Springer Nature remains neutral with regard to jurisdictional claims in published maps and institutional affiliations.

## Methods

**Fish rearing experiment.** *Acanthochromis polyacanthus* is a widespread and common Indo-Pacific damselfish. Breeding pairs lay demersal eggs, which hatch after 9–11 days. Fish were reared as previously described<sup>9</sup>. Briefly, offspring of eight wild-caught adult breeding pairs from the Palm Island region (18° 37' S, 146° 30' E) on the Great Barrier Reef, Australia, were reared for two generations at current-day ambient (+0°C) and +1.5°C or +3°C above ambient in a structured breeding design (Fig. 1a). The ambient and elevated temperature treatments followed a natural season cycle based on the 10-year temperature average for the study population (Australian Institute of Marine Science temperature loggers 6–8 m; <http://data.aims.gov.au/>). F<sub>1</sub> offspring were kept with their parents for 30 days post-hatching, at which time they were divided equally into three groups, of which two were gradually adjusted (>5 h) to +1.5°C and +3°C, while the third remained at the control temperature, +0°C. Temperature was kept within ±0.2°C of the desired treatment mean. Mortality was low, with >90% survival among sibling groups in all treatments. Sibling fish were kept in groups of 6 in 40 l aquaria for 1 year after hatching, at which time density was reduced to pairs. When fish reached maturity (at 1.5 years of age) they were randomly paired with a fish of the opposite sex from an unrelated family. Directly after hatching, F<sub>2</sub> individuals were removed from the parents and reared in 40 l aquaria at either control +0 or +3°C (Fig. 1a). This produced treatments of F<sub>2</sub> fish that were (1) reared from hatching at +0°C from parents maintained at +0°C control conditions, (2) reared from hatching at +3°C from parents maintained at +0°C control conditions, (3) reared from hatching at +3°C from parents maintained at +1.5°C, and (4) reared from hatching at +3°C from parents maintained at +3°C. Density of fish was decreased with development (see ref.<sup>11</sup> for details). Fish were reared in the treatments for approximately 2 years (that is, mature adults) when tissue sampling occurred. Breeding of F<sub>1</sub> individuals that developed in the +3°C conditions was skewed in the direction of one grandparental line<sup>2</sup>. Because F<sub>1</sub> breeding pairs were constructed with a random breeding design, stratified sampling of F<sub>2</sub> individuals was completed to gain the most consistent genetic diversity (linked back to the original 8 grandparental lines) across all treatments. Additionally, two males and two females were sampled from each of the treatments to control for the effects of gender on patterns observed. In only the step treatment differences were found depending on gender (Supplementary Table 6), and this was likely driven by sample S1 being distinct (Fig. 2c).

**Nucleic acids extraction and sequencing.** Whole livers of four to five adult fish from each treatment were dissected, immediately snap frozen in liquid nitrogen, and stored at –80°C until further processing. We chose to assess the methylome and transcriptome of the liver as it is a metabolically active organ and we are primarily interested in how *A. polyacanthus* adjusts metabolic performance following exposure to increased temperatures. To extract genomic DNA of each fish for genome and/or methylome sequencing, 100 mg of the snap frozen liver tissue was added to 700 µl CTAB (hexadecyltrimethylammonium bromide) buffer and homogenized. Proteinase K was added to the homogenate and incubated overnight at 55°C. RNase was added and left at room temperature for 10 min. This was followed by a standard chloroform/isoamyl alcohol extraction and ethanol precipitation<sup>33</sup>. DNA was suspended in TE buffer (10 mM Tris-Cl pH 8.0, 1 mM EDTA) and checked for quality and quantity on a 0.8% 1 × TBE gel.

An F<sub>1</sub> developmental fish from the same Palm Island population was used for the reference genome assembly (Supplementary Table 1). Five paired-end libraries were produced using the standard Illumina TruSeq protocol and seven mate-pair libraries with insert sizes ranging from 2.4 to 6.9 kb were produced using the standard Illumina Nextera and TruSeq protocol. These were sequenced for genome assembly on the Illumina HiSeq2000 platform by KAUST Bioscience core lab and Macrogen (Supplementary Table 1).

Whole genome bisulfite sequencing was conducted using Methyl-MaxiSeq Kit and Illumina HiSeq1500/2500 system by Zymo Research as follows: 500 ng of genomic DNA was digested with 2 units of Zymo Research's dsDNA Shearase Plus. The sheared fragments were end-blunted, A-extended at the 3' terminal end, and purified by Zymo Research's DNA Clean and Concentrate-5 kit according to the manufacturer's instructions. Pre-annealed adapters with 5'-methyl-cytosine were ligated to these fragments and then filled-in. Zymo Research's EZ DNA Methylation-Lightning kit was used for bisulfite treatment of the DNA fragments. Illumina TruSeq indices were used for polymerase chain reaction and the Agilent 2200 TapeStation was used to confirm the size and concentration of the fragments. Then, DNA fragments were sequenced on an Illumina HiSeq system.

Messenger RNA was extracted and sequenced as previously described<sup>9</sup>. Briefly, 400 µl aliquots of homogenized whole livers were applied to PerfectPure Preclear columns (5 Prime) and RNA was extracted according to the manufacturer's instructions, including an on-column DNAase treatment. Total RNA was sent to the Biosciences Core Laboratory sequencing facility at KAUST on an RNAsable plate (Biomatrica). cDNA synthesis and library construction were performed using the standard TruSeq protocol (Illumina) and HiSeq2000 was used for transcriptome sequencing.

**Assembly of genome and transcriptome sequences.** Raw genomic and transcriptomic reads were processed as previously described<sup>9</sup>.

Draft genome sequences were assembled de novo as follows: Contigs were assembled by ABySS v1.5.2<sup>34</sup> ( $k=65$ ) with default setting and then scaffolded using SSPACE v.3.06<sup>35</sup> with  $z$  (minimum contig size) = 200 and  $g$  (maximum allowed gaps for Bowtie) = 1. The assembled genome size was 992 Mb with 30,414 scaffolds (from 500 to 2,466,117 bp) and an N50 of 334,400 bp.

Completeness of genome assembly was assessed by CEGMA v.2.5<sup>36</sup>. 78.23% and 97.98% of 248 core eukaryotic genes were represented completely and partially, respectively.

To obtain base-level coverage of genome sequences, processed paired-end reads were aligned to the genomic scaffolds using Bowtie2 v.2.2.3<sup>37</sup> with '-X 1000 -sensitive' options. SAM files were sorted with SAMtools v.1.1<sup>38</sup> and genomeCoverageBed of BEDTools v.2.23<sup>39</sup> was applied to obtain base-level coverage. Coverage values for all bases were summed and divided by the genome length. This resulted in average coverage of 173×.

De novo transcriptome assembly was conducted with Trans-ABySS v.1.5.2<sup>40</sup> with  $k=32, 48, 64$  and 80. Reference-based transcriptome assembly was also performed using TopHat v.2.0.14<sup>41</sup> and Cufflinks v.2.2.1<sup>42</sup> with default parameters.

**Prediction of gene models and functional annotation.** Gene models were predicted with MAKER v.2.31.8<sup>43</sup>. For the mRNA evidence of gene annotation, de novo and reference-based assembled transcriptome sequences longer than 200 bp were merged and redundancy was removed using CD-HIT-EST v.4.6<sup>44</sup> with 95% identity. UniProtKB/Swiss-Prot<sup>45</sup> and CEGMA<sup>36</sup> core proteins were additionally used as protein evidence. SNAP v2006-07-28<sup>46</sup> and AUGUSTUS v3.0.3<sup>47</sup> were used as ab initio gene predictors. Repeats were annotated with RepeatMasker v.4.0.5<sup>48</sup>. Gene models with an annotation edit distance<sup>43</sup> score ≤ 0.75 were chosen. This resulted in 25,301 gene models with an average length of 2,466 bp for coding regions.

EMBOSS cpplot v.6.6.0.0<sup>49</sup> with default setting was adopted to identify CpG islands. 2 kb flanking sequences of CpG islands were defined as CpG island shores using slopBed of BEDTools v.2.23<sup>39</sup>. Promoters were defined as 2 kb upstream of transcription start sites using flankBed of BEDTools v.2.23<sup>39</sup>.

Homologues of gene models were annotated using BLASTP v.2.2.30<sup>50</sup> against the NCBI *nr* database ( $e$ -value cutoff:  $10^{-4}$ ).

**Analysis of DNA methylation and gene expression.** Raw methylomic reads were processed with Trim Galore! v.0.4<sup>51</sup> with the default setting and mapped to the genome sequences using Bismark v.0.13.1<sup>52</sup> with the default options and additionally the '-non\_directional' option. Methylome coverage per base was obtained using 'getCoverageStats' function of methylKit v.1.2.0<sup>53</sup>. Details of the resulting methylome dataset, including the percentage of methylated cytosines and methylome coverage are presented in Supplementary Table 2. DMRs for CpG, CHH, and CHG contexts were identified separately using the standard procedure of methylKit v.1.2.0<sup>53</sup>. Briefly, the 'methRead' function of methylKit reads the mapping results with 10 reads per cytosine as a minimum coverage threshold. High coverage bases (99.9%) were filtered to exclude potential PCR bias and then normalized using 'filterByCoverage' and 'normalizeCoverage' functions, respectively. Genomic regions were categorized as CpG island, CpG shore, promoter, 5' untranslated region (UTR), exon, introns, 3' UTR and repeats. Methylated or unmethylated cytosines in each genomic region were summed for each sample by the 'regionCounts' function of methylKit. The  $P$  values of methylation differences for each region between two samples were calculated using a chi-squared test in the 'calculateDiffMeth' function. To remove any influence of gender, male or female information was provided as a covariate argument in the 'calculateDiffMeth' function. We obtained  $q$ -values by collecting  $P$  values from all comparisons and adjusting them using the Benjamini–Hochberg method of the 'p.adjust' function. Genomic regions satisfying two criteria ( $q$ -value ≤ 0.05 and ≥ 25% methylation difference between two treatments) were considered as differentially methylated.

Heatmaps were generated using the 'heatmap.2' function of the 'gplots' package<sup>54</sup>. MDS analysis for DMRs was conducted using the 'mds' function of the 'smacof' R package<sup>55</sup> with '1 - Pearson correlation coefficient' as the dissimilarity measure. Confidence radii on MDS plots were calculated using the 'bootmds' function of the 'smacof' package<sup>55</sup> with 1,000 bootstrap replications. Quantification of separation between DMR sets from pairs of experimental groups (two-group planned comparisons) or between males and females within the same experimental groups was conducted using the 'rank.test' function of the 'ICSNP' package<sup>56</sup>. Resulting  $P$  values between treatments were adjusted with the Benjamini–Hochberg method of the 'p.adjust' function in R.

The closest gene to a DMR on the same scaffold was identified using 'closest' from BEDTools v.2.23<sup>39</sup>. This resulted in 1,563 genes from 2,078 CpG DMRs, while 115 DMRs were on scaffolds without annotated genes (Supplementary Table 4).

To quantify gene expression level, processed transcriptomic reads were aligned to the transcripts from gene models using Bowtie2 v.2.2.3<sup>37</sup> with '-X 1000 -sensitive' options. Resulting SAM files were sorted and converted to BAM files using SAMtools v.1.1<sup>38</sup>. Read counts per transcript were obtained using SAMtools idxstats<sup>38</sup>. DESeq2 v.1.6.3<sup>37</sup> was applied for normalization and detection of differentially expressed genes ( $q$ -value ≤ 0.05).

NAS was calculated as previously described<sup>10</sup>, whereby resting and maximum metabolic rate (RMR and MMR, respectively) of adult fish were measured at the

average summer temperature for each treatment (control = 28.5°C, developmental, step and transgenerational = 31.5°C) and NAS was calculated as the difference between MMR and RMR. Previously we have shown that acute exposure of adult control +0°C fish to +3°C (31.5°C) altered metabolic traits compared to developmental and transgenerational treatments<sup>2</sup>. Thus, as we did previously<sup>10</sup>, we standardized NAS by using the acute performance of the control fish to determine the expected metabolic response for NAS at 31.5°C with a linear regression. Using methylation levels of each genomic region and standardized NAS values from each fish (that is, not treatment averages), significant correlation was calculated as follows: methylation levels and standardized NAS values were shuffled 10 million times, respectively, and then Pearson correlation coefficients were calculated between shuffled methylation levels and standardized NAS values. This process was repeated until 1 million random correlation values were obtained. The 90% confidence interval was -0.423 to 0.427. Correlation values outside this range was regarded as significant correlation. Significant correlation between gene expression and standardized NAS was calculated in the same way. The 90% confidence interval was -0.386 to 0.38.

**Validation of high-throughput data.** Targeted bisulfite sequencing assays for CpG sites within selected DMRs was conducted by Zymo Research. Briefly, DNA samples from the same four individuals from each treatment used in the whole-genome bisulfite sequencing were used in the targeted bisulfite sequencing assay. As for the whole genome bisulfite sequencing, DNA was bisulfite-converted but then targeted regions were PCR-amplified. The PCR products were sequenced using MiSeq v.2 300 bp reagent kit and paired-end sequencing protocol. Sequenced reads were aligned to the reference genome sequences as described above, three technical replicates were produced for each individual, and reads from the same individual were merged. Aligned reads were analysed using the same methods for whole-genome bisulfite sequencing as described above. The 21 regions that had >10 reads in at least one CpG site were analysed for the validation of our results (Supplementary Table 9). All 21 regions showed statistical significance of differential methylation ( $q$ -value  $\leq 0.05$ ) and the same directional change of methylation with the results from whole-genome bisulfite sequencing. Moreover, 16 regions showed  $\geq 25\%$  methylation difference, indicating high accuracy in our results.

The quality of transcriptomes was previously validated using qRT-PCR<sup>3</sup>.

**Data availability.** Short reads from genome and methylome sequencing have been deposited in GenBank under BioProject ID [PRJNA348663](https://www.ncbi.nlm.nih.gov/bioproject/PRJNA348663). RNA-seq transcriptome sequences have been deposited in GenBank under BioProject ID [PRJNA255544](https://www.ncbi.nlm.nih.gov/bioproject/PRJNA255544).

## References

33. Sambrook, J. & Russell, D. W. *Molecular Cloning: A Laboratory Manual* 3rd edn (Cold Spring Harbor Laboratory Press, Cold Spring Harbor, 2001).
34. Simpson, J. T. et al. ABySS: a parallel assembler for short read sequence data. *Genome Res.* **19**, 1117–1123 (2009).
35. Boetzer, M., Henkel, C. V., Jansen, H. J., Butler, D. & Pirovano, W. Scaffolding pre-assembled contigs using SSPACE. *Bioinformatics* **27**, 578–579 (2011).
36. Parra, G., Bradnam, K. & Korf, I. CEGMA: a pipeline to accurately annotate core genes in eukaryotic genomes. *Bioinformatics* **23**, 1061–1067 (2007).
37. Langmead, B. & Salzberg, S. L. Fast gapped-read alignment with Bowtie 2. *Nat. Methods* **9**, 357–359 (2012).
38. Li, H. et al. The sequence alignment/Map format and SAMtools. *Bioinformatics* **25**, 2078–2079 (2009).
39. Quinlan, A. R. BEDTools: the Swiss-army tool for genome feature analysis. *Curr. Protoc. Bioinform.* **47**, 11–34 (2014). 11 12.
40. Robertson, G. et al. *De novo* assembly and analysis of RNA-seq data. *Nat. Methods* **7**, 909–912 (2010).
41. Kim, D. et al. TopHat2: accurate alignment of transcriptomes in the presence of insertions, deletions and gene fusions. *Genome Biol.* **14**, R36 (2013).
42. Trapnell, C. et al. Transcript assembly and quantification by RNA-Seq reveals unannotated transcripts and isoform switching during cell differentiation. *Nat. Biotechnol.* **28**, 511–515 (2010).
43. Holt, C. & Yandell, M. MAKER2: an annotation pipeline and genome-database management tool for second-generation genome projects. *BMC Bioinform.* **12**, 491 (2011).
44. Li, W. & Godzik, A. Cd-hit: a fast program for clustering and comparing large sets of protein or nucleotide sequences. *Bioinformatics* **22**, 1658–1659 (2006).
45. Boutet, E., Lieberherr, D., Tognolli, M., Schneider, M. & Bairoch, A. UniProtKB/Swiss-Prot. *Methods Mol. Biol.* **406**, 89–112 (2007).
46. Korf, I. Gene finding in novel genomes. *BMC Bioinform.* **5**, 59 (2004).
47. Stanke, M., Steinkamp, R., Waack, S. & Morgenstern, B. AUGUSTUS: a web server for gene finding in eukaryotes. *Nucleic Acids Res.* **32**, W309–W312 (2004).
48. Tarailo-Graovac, M. & Chen, N. Using RepeatMasker to identify repetitive elements in genomic sequences. *Curr. Protoc. Bioinform.* **25**, 4.10.1–4.10.14 (2009).
49. Li, W. et al. The EMBL-EBI bioinformatics web and programmatic tools framework. *Nucleic Acids Res.* **43**, W580–W584 (2015).
50. Altschul, S. F., Gish, W., Miller, W., Myers, E. W. & Lipman, D. J. Basic local alignment search tool. *J. Mol. Biol.* **215**, 403–410 (1990).
51. Krueger F. Trim Galore! v.0.4 (Babraham Bioinformatics, 2015); [http://www.bioinformatics.babraham.ac.uk/projects/trim\\_galore](http://www.bioinformatics.babraham.ac.uk/projects/trim_galore)
52. Krueger, F. & Andrews, S. R. Bismark: a flexible aligner and methylation caller for Bisulfite-Seq applications. *Bioinformatics* **27**, 1571–1572 (2011).
53. Akalin, A. et al. methylKit: a comprehensive R package for the analysis of genome-wide DNA methylation profiles. *Genome Biol.* **13**, R87 (2012).
54. Warnes, G. R. et al. *gplots: various R programming tools for plotting data* R package v.3.0.1 (R Foundation, 2016); <http://CRAN.R-project.org/package=gplots>
55. De Leeuw, J. & Mair, P. Multidimensional scaling using majorization: SMACOF in R. *J. Stat. Softw.* **31**, i03 (2009).
56. Nordhausen, K., Sirkia, S., Oja, H. & Tyler, D. ICSNP: *Tools for Multivariate Nonparametrics* R package v.1.1-0. (R Foundation, 2015).
57. Love, M. I., Huber, W. & Anders, S. Moderated estimation of fold change and dispersion for RNA-seq data with DESeq2. *Genome Biol.* **15**, 550 (2014).